This is a peer-reviewed, author's accepted manuscript of the following conference output:
McAlorum, J., Vlachakis, C., & Perry, M. (2021). A low-cost electrical impedance analyser for interrogating self-sensing cement repairs. In 2021 IEEE International Instrumentation and Measurement Technology Conference (I2MTC) (pp. 1-6). IEEE.
https://doi.org/10.1109/i2mtc50364.2021.9459871

A low-cost electrical impedance analyser for interrogating self-sensing cement repairs

1st Jack McAlorum
Civil & Environmental Engineering
University of Strathclyde
Glasgow, UK
jack.mcalorum@strath.ac.uk

2nd Christos Vlachakis
Civil & Environmental Engineering
University of Strathclyde
Glasgow, UK

3rd Marcus Perry
Civil & Environmental Engineering
University of Strathclyde
Glasgow, UK

***Abstract*—In this paper, we showcase initial results from a bespoke, low-cost interrogator for complex impedance measurements of our robotically deployed self-sensing cement (geopolymer) technology for concrete monitoring and maintenance. Our low-cost (£30, $40 USD) interrogation system is benchmarked against the performance of a £12k ($16k USD) commercially available lab-spec electrical impedance analyser. Results show the low-cost interrogator is able to match the commercial interrogation system well-enough for the field measurement of impedance, with an impedance root mean square error (RMSE) of $\pm$5.4 % for an ideal cell. For pure geopolymer samples, similar results are found, with an RMSE of $\pm$5.2 %. During patch measurements, although non-linearity was witnessed, the low-cost interrogator showcased the ability to measure the impedance and impedance-frequency variations. Therefore, the first iteration of low-cost interrogator design shows promise for monitoring geopolymer self-sensing repair complex impedances in the field.**

***Index Terms*—low-cost interrogator, complex impedance measurement,multi-functional materials, self-sensing repair, robotic deployment.**

I. Introduction

Driven by ageing concrete in various industries; an abundance of innovative research has produced many unique approaches to concrete maintenance and monitoring. Sensors for crack detection in existing concrete vary from electrical-based sensors [1]–[3] to complex and fragile optical fibre networks [4]–[6] and even non-destructive wave propagation techniques [7]–[9]. Advances in concrete repairs focus on low-carbon alternatives such as using geopolymers (a class of alkali-activated materials) with fly-ash [10], steel slag [11] or metakaolin [12] pre-cursors. These materials are not only environmentally friendly, but also present comparable bond strengths to conventional repairs [13]–[15]. Recently, utilization of these materials inherent conductive properties have granted temperature, chloride and strain sensing capabilities; in-addition to their repair properties [16]–[18].

A common denominator in the previous examples is manual deployment of the technologies. Generally, there are three distinct issues with manual deployment:

- Personnel safety - especially in hazardous environments such as at nuclear stations.
- Workmanship - repeatability and robustness of installation, such as bond strength of repairs, are dependant on human ability and any errors they make.
- Cost - varying labour productivity can cause high unpredictable costs.

In future, automated deployment could seek to address these issues by providing consistent and autonomous installations at a fixed cost regardless of the environment.

In recent work, we have demonstrated the capability of both 3D printing [19] and robotic spray coating [20] of a metakaolin geopolymer for concrete non-structural repair with temperature and strain self-sensing capabilities. Impedance measurements were taken using a commercially available electrochemical impedance analyser. The cost of such a lab-spec device is approximately £12k ($16k USD). In a widescale field trial, a multitude of sensor-repair patches is desirable. This would require multiple interrogation systems. Therefore; a low-cost alternative for field deployment is essential for a cost efficient maintenance and monitoring system.

Low-cost interrogators for complex impedance measurement have been researched over the years. Butterworth et al. [21] developed a low-cost potentiostat for 3 electrode measurement of micro-biological resistances. In the case of civil applications, Corva et al. [22] developed a linear 4-probe impedance measurement device for embedding into concrete for chloride measurement. The objective of the work in this paper is to demonstrate the capability of complex impedance interrogation of self-sensing geopolymer using a low-cost custom built circuit. Comparisons between this circuit and a commercially available system are performed.

II. Methodology

A. Geopolymer design

Geopolymers comprise of an aluminosilicate solid, usually metakaolin, fly-ash or slag, rigorously mixed with an alkaline sodium-based solution [23], [24]. The outcome is a cementitious material that cures similar to a portland-based cement and has comparable mechanical properties [25], [26]. As discussed, exploiting this has provided low-carbon concrete repair alternatives. Geopolymers also contain an inherent conductivity providing a piezoresistive behaviour [27] that is dependant on

This work was funded in part by the Advanced Nuclear Research Centre (ANRC-27), and the Scottish Funding Council's Oil & Gas Technology Centre.

measurands such as temperature, moisture, chloride and strain [28], [29].

In this work, kaolin is calcined at 800 °C for 2 hours to produce metakaolin. This is then mixed with a 2:1 sodium silicate:hydroxide solution at a mass ratio of 0.65 solid:liquid. This ratio is relatively low compared to reported mixes [30]; however, to obtain a sprayable material a more workable mix is required. In order to combat shrinkage cracking that can occur post-cure [31], 3 mm long polyvinyl acetate (PVA) fibres at 0.1% of solid weight were added. It is common to introduce additives in to geopolymer mixes depending on the requirement. For example - sand is added to improve compressive strength [32] and plasticisers can be added to increase workability [33].

B. Robotic spray coating

For an extensive presentation of our work on robotic spray-coating of geopolymers, see [20]. Since the subject of this paper is interrogating the geopolymer patches, only a short overview of the deployment process will be provided. The mix design given in Section II-A has been developed to allow precise robotic spray-coating on to concrete. The precision spray-coater is attached to a robotic arm, pictured in Fig. 1. The robot program can be customised for various shapes and sizes of patch. To be consistent, a small square patch of 50 x 50 mm was chosen. The geopolymer is sprayed on to a post-30 day cured portland cement-based concrete sample before electrodes are inserted. The sample is covered and cured at 40 °C for 48 hours concluding in a patch as shown in Fig. 2.

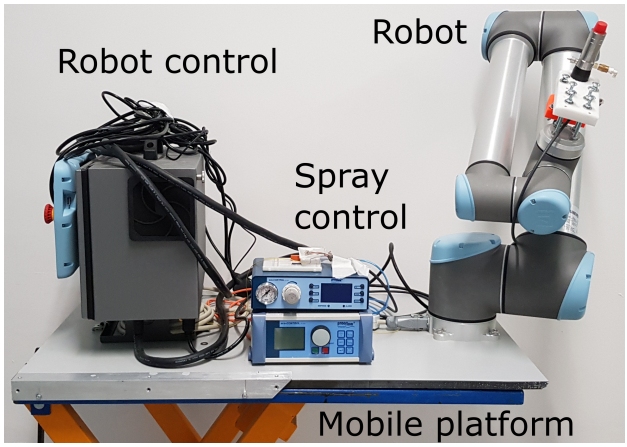

Fig. 1. Mobile robotic spray-coating rig.

C. Interrogation principles

A complex impedance, Z can comprise of a resistance (R), a capacitance (X_C) and/or an inductance (X_L), given as:

$$Z = R + X_C + X_L \tag{1}$$

From basic principles, the impedance can be calculated from time-dependant applied voltage potential, ($V_a(t)$) and current, ($I_a(t)$):

Fig. 2. Small spray-coated geopolymer patch.

$$Z = \frac{V_a(t)}{I_a(t)} \tag{2}$$

However, since X_C and X_L are frequency dependant components, the applied voltage/current must be AC, otherwise the complex impedance cannot be measured (for DC: $X_C \to \infty, X_L \to 0$). Therefore:

$$Z = \frac{|V_a|}{|I_a|} e^{j\Theta} \tag{3}$$

where $|V_a|$ and $|I_a|$ are the amplitudes of the voltage and current waveforms respectively. Θ is the phase or time (ΔT) difference between current and voltage, when applied at frequency, f where:

$$\Theta = 360 f \Delta T \tag{4}$$

and the impedance modulus, $|Z|$ is given as:

$$|Z| = \frac{|V_a|}{|I_a|} \tag{5}$$

Generally, a sweep of frequencies, for example: 100 Hz - 100 kHz, is applied to gain a comprehensive impedance modulus measurement against frequency, such as in Figure 3. This is known as a Bode plot in Electrochemical Impedance Spectroscopy (EIS).

In electrochemistry, the impedance of an electrochemical cell is usually measured using 3 or 4 electrodes. A 4 electrode set up is preferred when the main measurand is the impedance of the body, rather than any reactions occurring at the electrodes. Since in this work, it is desired to remove any electrode-sample interactions - 4 electrode measurement is used, as shown in Figure 4. A sinusoidal voltage/current (V_a/I_a) of frequency, f is applied over two electrodes and a voltage (V_m) is measured over the other two. This now gives:

$$|Z| = \frac{|V_m|}{|I_a|} \tag{6}$$

Therefore, for a low-cost interrogation scheme, the ability to apply a varying frequency sinusoidal voltage/current and to measure a second voltage is required.

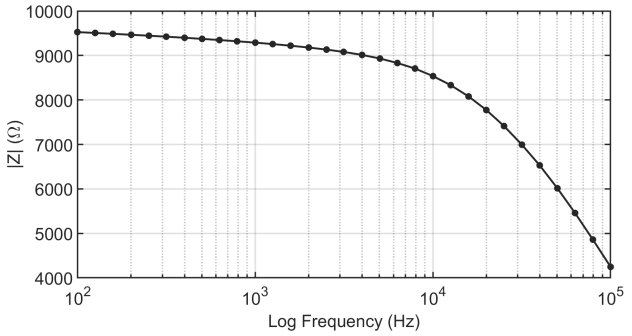

Fig. 3. A typical Bode plot for a electrochemical cell: impedance modulus $|Z|$ is dependant on frequency of applied voltage/current.

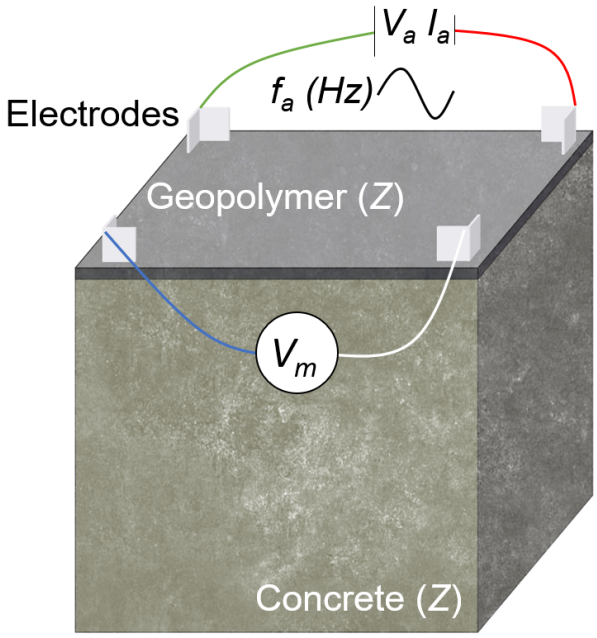

Fig. 4. Four electrode set up for complex impedance measurement of geopolymer patch. Impedance measurement, Z of geopolymer may be influenced by concrete. Z is gained by measuring a voltage, V_m and the applied current I_a.

D. Low-cost interrogator

A simplified block diagram for the low-cost interrogator circuit is given in Fig. 5. To achieve the requirements set out in Section II-C, a circuit has been designed using an Atmel ATXMEGA128A4U microcontroller (MCU). This particular chip was chosen for a few reasons:

- Large memory - communication is usually slow, so saving to onboard memory prior to transmission can allow for faster voltage application and faster testing in general
- High speed digital-to-analogue converter (DAC) for applying voltage
- Multiple high speed analogue-to-digital converters (ADCs) for measuring voltage/current
- High number of digital outputs will allow for multiplexing for future work

To keep costs low, the single MCU is used to perform all tasks: application, measurement, storage and communication via UART (Universal Asynchronous Receiver/Transmitter) to a computer. Any additional modules can always be introduced later when bottlenecks are reached or requirements change. A single DAC is used to apply a sinusoidal voltage of 0.2 V using a lookup table of 20 samples. This voltage is shifted using a voltage divider (V_{shift}) to apply $\pm$ 0.1 V to the sample across pins 1 and 2. A single TLC2262 chip with two amplifiers is used for amplification. Firstly, since the ADC can only measure voltage, a measurement resistor, R_m is used to convert current from pin 2 to a voltage. This is then amplified/de-amplified as required using a variable gain. This is converted back in post-production using:

$$I_a = \frac{\frac{V_{ADC1}}{A_{Amp1}}}{R_m} \tag{7}$$

where V_{ADC1} is the voltage on the MCU ADC1 and A_{AMP1} is the variable gain of amplifier AMP1. The second amplifier, AMP2 is used to sum the voltages from pins 3 and 4 to give V_m on ADC2. The geopolymer impedance is then calculated using eq. 6.

The MCU in this work is capable of performing a single DAC 12-bit conversion every $\approx$ 7 μs and ADC 12-bit conversion every $\approx$ 3.5 μs [34]. For a 20 sample sinusoid, this means the absolute maximum frequency the circuit can apply is $\approx$ 4 kHz. With the addition of saving measurements to memory and general processing requirements (integer incrementation, looping etc.) the actual value will be less. In fact, during testing the maximum frequency achievable was 1.2 kHz. This is acceptable, as measuring a single frequency over time is adequate for the current application. However, there are a multitude of ways to increase this frequency. For example - a separate voltage application circuit would allow a 14 kHz sinusoid to be sampled. This avenue may be explored in future work, if a greater frequency is required.

The overall cost of the entire circuit pre-PCB printing is $\approx$ £30 ($40 USD). The printing costs us an additional £20 at low volumes, but varies by quantity, lead time and locale. Bulk buying components and PCBs would reduce the price significantly.

E. Experimental set up

To examine the initial capabilities of the low-cost interrogator, these experiments are independent of measurands, i.e. at an equilibrium state. Samples are measured using the commercial interrogator first, then the low-cost system, before a second measurement is taken using the commercial interrogator to ensure impedance is constant.

Two measurement methods were used. For EIS, a single sweep of $\pm$ 0.1 V AC sinusoidal voltage from 100 Hz - 1.2 kHz is performed over 200 steps, as previously explained. The impedance is calculated post-measurement using eq. 6. This method was carried out for various pure geopolymer samples - i.e. not patches on concrete. In the case of concrete patches, it was discovered that impedances were relatively constant

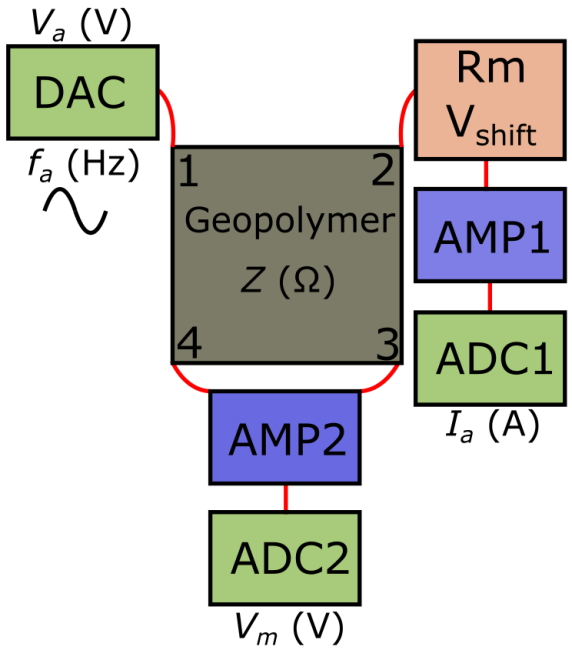

Fig. 5. Simplified block diagram of circuit operation: MCU provides a sinusoid voltage via on-board DAC, V_a, at frequency, f_a to a geopolymer of complex impedance, Z. Measurements are made using the MCUs ADCs for the applied current, I_a, and measured voltage, V_m.

over the short range of frequencies the circuit can apply, meaning the low-cost interrogator was unable to distinguish these variations. Therefore, during testing of these samples only the two extreme frequency measurements were taken (1 Hz and 1.2 kHz).

1) Randles cell: In the first experiment, a Randles cell was used to calibrate the instruments. A Randles cell, shown in Fig. 6, is an ideal representation of a complex impedance cell using known electrical components. Since the impedance can be calculated mathematically, the commercial interrogator measurement can also be verified. To remove errors due to resistor tolerances, impedance measurements are normalized to between 0 and 1. This provides a more accurate comparison between the interrogators, as the relative change in impedance due to frequency can be identified.

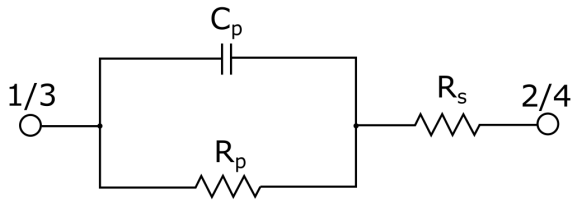

Fig. 6. Randles cell used in this work: C_p = 1.2 μF, R_p = 3 kΩ and R_s = 247 Ω. Total impedance at 1 kHz = 398.2 Ω.

2) Geopolymer samples: As mentioned, two types of geopolymer samples were tested: pure geopolymer blocks (shown in Fig. 7) and concrete geopolymer patches (shown in Fig. 2). A total of seven geopolymer block impedances were measured over the frequencies 100 - 1.2 kHz using both interrogation systems. Eight patches were then measured using two frequencies (100 Hz and 1.2kHz).

Fig. 7. Pure geopolymer block with protruding electrodes.

III. Results and Discussion

A. Randles Cell

An EIS sweep from 100 Hz - 1.2 kHz was performed using both interrogators. Fig. 8 a) shows the bode plots gained, where impedance modulus has been normalized. It is apparent that the general trend of impedance change with frequency is adequately measured by the low-cost interrogator. As expected, the commercial interrogator is extremely accurate in measuring the impedance, whereas the low-cost displays a clear measurement error. Although this error looks greater at low impedance, when commercial vs. low-cost is plot (compensating for any variation in frequency) as in Fig. 8 b), it is clear the error is relatively constant. From this figure, a somewhat linear relationship is observed. Fitting a linear trend and calculating the root mean square error (RMSE) gives ± 0.0544 or $\approx \pm$ 5.4%.

B. Pure geopolymer

Similarly, a single EIS sweep of 100 Hz - 1.2 kHz was taken for each pure geopolymer sample. Impedance, $|Z|$ for these samples range from 100 Ω to 3 kΩ. Fig. 10 a) shows the bode plot for sample 4 for both interrogators. Fig. 10 b) again shows the normalized $|Z|$, Z_{norm} of commercial vs. low-cost. From the bode plot, a), it is clear the low-cost is again able to distinguish the impedance variation with frequency and matches well with the commercial trend. From the impedance plot, b), a linear relationship is again apparent between the two interrogators for every sample (1-7), with a relatively constant RMSE over the entire sweep of $\approx \pm$ 5.2%. For a first iteration of the low-cost interogator design this is a promising result. Of course, improvements to reduce this error will be essential before the interrogator is ready for field deployment.

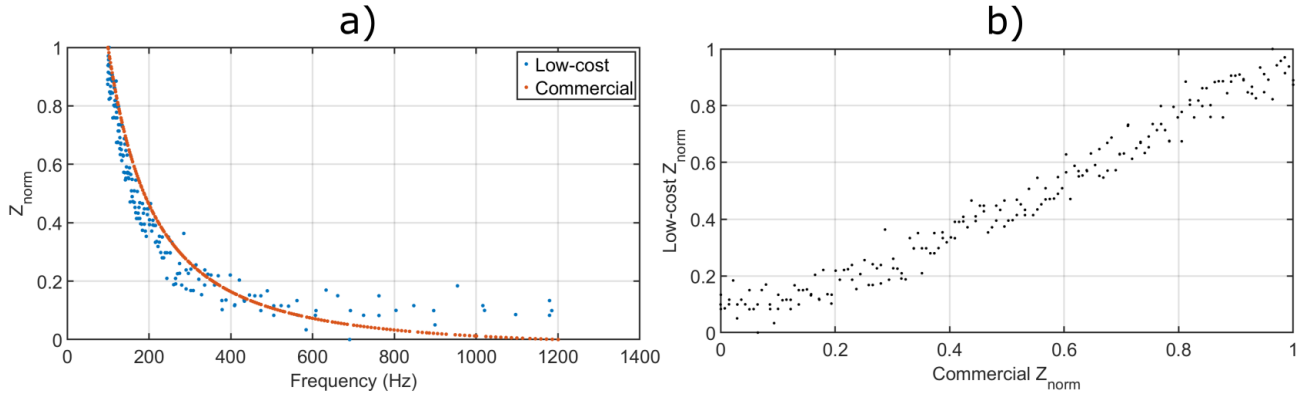

Fig. 8. Results from interrogator comparison of EIS sweep from 1 Hz to 1.2 kHz on Randles cell. In a), the bode plot of both interrogators with normalized $|Z|$, Z_{norm} vs. frequency. In b) Z_{norm} of commercial vs. low-cost shows a linear relationship. Calculated RMSE is $\approx \pm$ 5.4%.

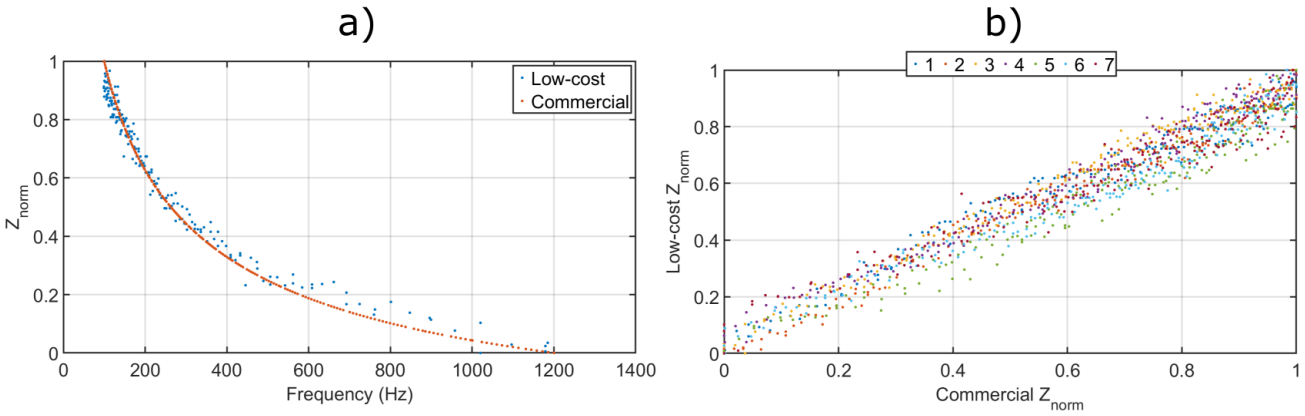

Fig. 9. Results from interrogator comparison of EIS sweep from 1 Hz to 1.2 kHz on seven pure geopolymer blocks. Graph a) shows the bode plot for sample 4 from both interrogators, b) shows the normalized $|Z|$, Z_{norm} of commercial vs. low-cost for each sample (1-7). Similarly to the Randles cell, a linear relationship is observed, with calculated RMSE $\approx \pm$ 5.2%.

C. Geopolymer patch

As discussed, current capable sweep range is unsuitable for patches as impedance variation is small. Impedance, $|Z|$ for these samples range from 6.4 kΩ to 13 kΩ. Two measurements were taken with both interrogators at 100 Hz and 1.2 kHz for each of the eight patches. A plot of normalized impedance modulus, Z_{norm} for commercial vs. low-cost is shown in Fig. 10. Unlike the previous experiments, a linear relationship is not apparent. Each sample is illustrated by a "pair" of points on the graph, representing the two applied frequencies. Clearly, even on the commercial measurements the variation between 100 Hz and 1.2 kHz is small. However, the low-cost is also able to distinguish this change in most samples. Promisingly, the general upward trend of sample impedance is matched by the low-cost interrogator, but clearly some non-linearity is witnessed. It is assumed, due to the increased impedance compared to the pure geopolymer blocks, in addition to the introduction of concrete, a negative affect on the accuracy of the low-cost interrogator has occurred. Essentially, the measurement error in this case is impedance dependant, with a larger error with increased impedance. For these samples, measurement resistor R_m was increased relative to the increase of impedance. Possibly this method of current measurement needs reviewing and altered for larger impedance measurements. This will be studied in greater detail in future work.

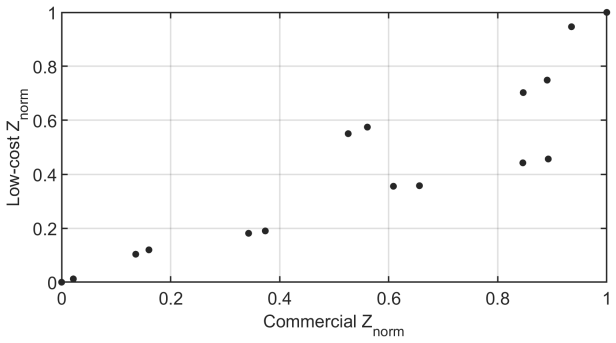

Fig. 10. Normalized $|Z|$, Z_{norm} of commercial vs. low-cost interrogator. Point "pairs" represent the two frequency measurements of each sample. General upwards trend is matched by the low-cost interrogator, as well as the small variation due to frequency. However, non-linearity is apparent and work will be required to rectify this.

IV. Conclusion

In this paper, a low-cost interrogation system for complex impedance measurement of self-sensing geopolymers is demonstrated and compared to a commercially available system. An ideal circuit representation of an elctrochemical cell produced results concluding in an $\approx \pm$ 5.4% RMSE between the low-cost and commercial interrogator. Pure geopolymer samples replicate this result, with an RMSE of $\approx \pm$ 5.2%. Moving to geopolymer patches on concrete, however, showed some non-linearity in the comparison. Low-cost measurements still followed a general linear trend, but error was much greater for higher impedances. Overall, considering this is a first iteration of the interrogation system, results are promising for use as a field deployed interrogation system for geopolymer patches. Future work should focus on reviewing the circuit design with the objective of monitoring patches of higher impedance with a lower error compared to the commercial interrogator.

Acknowledgment

References

[1] Z. Zhou *et al.*, "Smart film for crack monitoring of concrete bridges," *Structural health monitoring*, 2010.

[2] N. A. Hoult, P. R. A. Fidler, P. G. Hill, and C. R. Middleton, "Long-term wireless structural health monitoring of the ferriby road bridge," *Journal of Bridge Engineering*, 2010.

[3] J. Yan, A. Downey, A. Cancelli, S. Laflamme, A. Chen, J. Li, and F. Ubertini, "Concrete crack detection and monitoring using a capacitive dense sensor array," *Sensors*, vol. 19, no. 8, 2019. [Online]. Available: https://www.mdpi.com/1424-8220/19/8/1843

[4] R. A. Silva-Muñoz and R. A. Lopez-Anido, "Structural health monitoring of marine composite structural joints using embedded fiber Bragg grating strain sensors," *Composite Structures*, vol. 89, no. 2, pp. pp. 224–234, 2009.

[5] M. Perry, J. McAlorum, G. Fusiek, I. McKeeman, T. Rubert, and P. Niewczas, "Crack monitoring of operational wind turbine foundations," *MDPI Sensors*, vol. 17, 2017.

[6] J. McAlorum, T. Rubert, G. Fusiek, P. Niewczas, and G. Zorzi, "Design and demonstration of a low-cost small-scale fatigue testing machine for multi-purpose testing of materials, sensors and structures," *Machines*, July 2018. [Online]. Available: http://www.mdpi.com/2075-1702/6/3/30

[7] D. G. Aggelis, E. Z. Kordatos, D. V. Soulioti, and T. E. Matikas, "Combined use of thermography and ultrasound for the characterization of subsurface cracks in concrete," *Construction and Building Materials*, vol. 24, no. 10, pp. pp. 1888–1897, 2010.

[8] D. G. Aggelis, E. Z. Kordatos, M. Strantza, D. V. Soulioti, and T. E. Matikas, "NDT approach for characterization of subsurface cracks in concrete," *Construction and Building Materials*, vol. 25, no. 7, pp. pp. 3089–3097, 2011.

[9] Y.-Z. Song, C. R. Bowen, A. H. Kim, A. Nassehi, J. Padget, and N. Gathercole, "Virtual visual sensors and their application in structural health monitoring," *Structural Health Monitoring*, vol. 13, no. 3, pp. pp. 251–264, 2014. [Online]. Available: http://shm.sagepub.com/content/early/2014/02/17/1475921714522841\nhttp://urmassn11.ijdo.org/papers/urmassn11_submission_71.pdf

[10] T. Phoo-ngernkham, V. Sata, S. Hanjitsuwan, C. Ridtirud, S. Hatanaka, and P. Chindaprasirt, "High calcium fly ash geopolymer mortar containing portland cement for use as repair material," *Construction and Building Materials*, vol. 98, pp. 482 – 488, 2015. [Online]. Available: http://www.sciencedirect.com/science/article/pii/S0950061815303561

[11] S. Hu, H. Wang, G. Zhang, and Q. Ding, "Bonding and abrasion resistance of geopolymeric repair material made with steel slag," *Cement and Concrete Composites*, vol. 30, no. 3, pp. 239 – 244, 2008. [Online]. Available: http://www.sciencedirect.com/science/article/pii/S0958946507000662

[12] Z. Zhang, X. Yao, and H. Wang, "Potential application of geopolymers as protection coatings for marine concrete iii. field experiment," *Applied Clay Science*, vol. 67-68, pp. pp. 57 – 60, 2012, clay and Water Treatment. [Online]. Available: http://www.sciencedirect.com/science/article/pii/S0169131712001548

[13] W. W. Zailani, A. Bouaissi, M. Mustafa, M. M. A. B. Abdullah, R. Razak, S. Yoriya, M. A. A. Mohd Salleh, A. Salleh, R. Mohd, M. Rozainy, and H. Fansuri, "Bonding strength characteristics of fa-based geopolymer paste as a repair material when applied on opc substrate," *Applied Sciences*, vol. 10, p. 3321, 05 2020.

[14] S. Hu, H. Wang, G. Zhang, and Q. Ding, "Bonding and abrasion resistance of geopolymeric repair material made with steel slag," *Cement and Concrete Composites*, vol. 30, no. 3, pp. 239 – 244, 2008. [Online]. Available: http://www.sciencedirect.com/science/article/pii/S0958946507000662

[15] C. Zanotti, P. H. Borges, A. Bhutta, and N. Banthia, "Bond strength between concrete substrate and metakaolin geopolymer repair mortar: Effect of curing regime and pva fiber reinforcement," *Cement and Concrete Composites*, vol. 80, pp. 307 – 316, 2017. [Online]. Available: http://www.sciencedirect.com/science/article/pii/S0958946516304590

[16] M. Perry, M. Saafi, G. Fusiek, and P. Niewczas, "Geopolymeric thermal conductivity sensors for surface-mounting onto concrete structures," *9th International Concrete Conference 2016: Environment, Efficiency and Economic Challenges for Concrete*, 2016. [Online]. Available: https://strathprints.strath.ac.uk/id/eprint/60745

[17] M. Saafi, A. Gullane, B. Huang, H. Sadeghi, J. Ye, and F. Sadeghi, "Inherently multifunctional geopolymeric cementitious composite as electrical energy storage and self-sensing structural material," *Composite Structures*, vol. 201, pp. pp. 766 – 778, 2018. [Online]. Available: http://www.sciencedirect.com/science/article/pii/S0263822318312431

[18] L. Biondi, M. Perry, J. McAlorum, C. Vlachakis, and A. Hamilton, "Geopolymer-based moisture sensors for reinforced concrete health monitoring," *Sensors and Actuators B: Chemical*, vol. 309, no. 127775, 2020. [Online]. Available: http://www.sciencedirect.com/science/article/pii/S0925400520301222

[19] C. Vlachakis, M. Perry, L. Biondi, and J. McAlorum, "3d printed temperature-sensing repairs for concrete structures," *Additive Manufacturing*, vol. 34, no. 101238, 2020. [Online]. Available: http://www.sciencedirect.com/science/article/pii/S2214860420306102

[20] J. McAlorum, M. Perry, C. Vlachakis, L. Biondi, and B. Lavoie, "Robotic spray coating of self-sensing metakaolin geopolymer for concrete monitoring," *Automation in Construction*, vol. 121, p. 103415, 2021. [Online]. Available: http://www.sciencedirect.com/science/article/pii/S092658052030995X

[21] A. Butterworth, D. K. Corrigan, and A. C. Ward, "Electrochemical detection of oxacillin resistance with simplestat: a low cost integrated potentiostat and sensor platform," *Anal. Methods*, vol. 11, pp. 1958–1965, 2019. [Online]. Available: http://dx.doi.org/10.1039/C9AY00383E

[22] D. M. Corva, S. S. Hosseini, F. Collins, S. D. Adams, W. P. Gates, and A. Z. Kouzani, "Miniature resistance measurement device for structural health monitoring of reinforced concrete infrastructure," *Sensors*, vol. 20, no. 15, 2020. [Online]. Available: https://www.mdpi.com/1424-8220/20/15/4313

[23] J. Davidovits, "Geopolymers: inorganic polymeric new materials," *Thermal analysis*, vol. 37, 1991.

[24] J. L. Provis, "Geopolymers and other alkali activated materials: Why, how and what?" *Materials and structures*, vol. 47, 2014.

[25] R. Pouhet and M. Cyr, "Formulation and performance of flash metakaolin geopolymer concretes," *Construction and Building Materials*, vol. 120, pp. pp. 150 – 160, 2016. [Online]. Available: http://www.sciencedirect.com/science/article/pii/S0950061816307863

[26] R. Pouhet, M. Cyr, and R. Bucher, "Influence of the initial water content in flash calcined metakaolin-based geopolymer," *Construction and Building Materials*, vol. 201, pp. pp. 421 – 429, 2019. [Online]. Available: http://www.sciencedirect.com/science/article/pii/S0950061818331994

[27] C. Lamuta, L. Bruno, S. Candamano, and L. Pagnotta, "Piezoresistive characterization of graphene/metakaolin based geopolymeric mortar composites," *MRS Advances*, vol. 2, pp. pp. 1–7, 11 2017.

[28] P. Rovnaník, I. Kusák, P. Bayer, P. Schmid, and L. Fiala, "Comparison of electrical and self-sensing properties of portland cement and alkali-activated slag mortars," *Cement and Concrete Research*, vol. 118, pp. pp. 84 – 91, 2019. [Online]. Available: http://www.sciencedirect.com/science/article/pii/S0008884618303429

[29] P. Duxson, A. Fernández-Jiménez, J. L. Provis, G. C. Lukey, A. Palomo, and J. S. J. van Deventer, "Geopolymer technology: the current state of the art," *Journal of Materials Science*, vol. 42, no. 9, pp. 2917–2933, May 2007. [Online]. Available: https://doi.org/10.1007/s10853-006-0637-z

[30] L. Chen et al., "Preparation and properties of alkali activated metakaolin-based geopolymer," *Materials*, 2016.

[31] C. Kuenzel, L. J. Vandeperre, S. Donatello, A. R. Boccaccini, and C. Cheeseman, "Ambient temperature drying shrinkage and cracking in metakaolin-based geopolymers," *Journal of the American Ceramic Society*, vol. 95, no. 10, pp. pp. 3270–3277, 2012. [Online]. Available: https://ceramics.onlinelibrary.wiley.com/doi/abs/10.1111/j.1551-2916.2012.05380.x

[32] X. Li, F. Rao, S. Song, M. A. Corona-Arroyo, N. Ortiz-Lara, and E. A. Aguilar-Reyes, "Effects of aggregates on the mechanical properties and microstructure of geothermal metakaolin-based geopolymers," *Results in Physics*, vol. 11, pp. 267 – 273, 2018. [Online]. Available: http://www.sciencedirect.com/science/article/pii/S2211379718319405

[33] L. Carabba, S. Manzi, and M. C. Bignozzi, "Superplasticizer addition to carbon fly ash geopolymers activated at room temperature," *Materials*, vol. 9, no. 7, 2016. [Online]. Available: https://www.mdpi.com/1996-1944/9/7/586

[34] Microchip, "Atxmega128a4u data sheet," last visited: Oct. 2020. [Online]. Available: https://www.microchip.com/wwwproducts/en/ATxmega128A4U